WET-CHEMICAL SYNTHESIS OF APATITE-BASED CERAMIC WASTE FORMS FOR THE IMMOBILIZATION OF RADIOACTIVE IODINE (I-129)

By

CHARLES EN HUA CAO

A thesis submitted to the

Graduate School-New Brunswick

Rutgers, The State University of New Jersey

In partial fulfillment of the requirements

For the degree of

Master of Science

Graduate Program in Materials Science and Engineering

Written under the direction of

Ashutosh Goel

And approved by

_____

_____

_____

New Brunswick, New Jersey

January 2017

ABSTRACT OF THE THESIS

Wet-Chemical Synthesis of Apatite-Based Ceramic Waste Forms for the Immobilization of Radioactive Iodine (I-129)

By CHARLES EN HUA CAO

Thesis Director:
Ashutosh Goel

One of the key components to a feasible and sustainable nuclear fuel cycle is a viable set of waste forms for the radionuclides and fission products. Of particular concern are the highly volatile radionuclides such as iodine – 129. The current proposed technology for the removal of iodine from reprocessing plant off-gas is to pass it through a bed of silver solid sorbents (i.e. silver zeolite) to form chemisorbed AgI and/or bubble the off-gas into a caustic solution. At this point in time, this iodine capture media is being stored on waste treatment facilities awaiting a viable waste form solution for storage into a geological repository. Iodine is not amenable to conventional borosilicate vitrification routes because of its low solubility in some glass chemistries and, more importantly, its high volatility at typical glass processing temperatures (1000 - 1100°C). Therefore, considerable effort is being made to develop alternative waste forms for iodine. However, most proposed waste forms to date have not achieved sufficient maturity and satisfactory properties (specifically: ease of processing, high waste loading, and high chemical durability) to be considered as promising technologies.

Apatite-based ceramic waste forms have been considered as potential candidates for immobilization of radioactive iodine for a long time. In particular, lead vanadate based apatite minerals [i.e. $Pb_{10}(VO_4)_6I_2$] have been suggested as promising waste forms in this regard mainly due to their ability to accommodate iodine in their crystal structure. Although promising, the

major challenges associated with these minerals are either high processing temperatures along with complicated synthesis routes or poor chemical durability. While the concerns pertaining to poor chemical durability of these minerals have been addressed by partial substitution of vanadate $(VO_4)_3$- by phosphate $(PO_4)_3$- ions $[Pb_{10}(VO_4)_{6-x}(PO_4)_xI_2]$, as investigated in literature, the high processing temperatures and complicated synthesis routes of these minerals still pose a big challenge for the continuous mass production of these waste forms.

In this study, we present the first reported instance of wet-chemical synthesis of the well-known apatite, $Pb_{10}(VO_4)_6I_2$. By being able to utilize wet-chemical synthesis, the ability to scale up the production of an iodine-containing apatite to an industrial level is made possible and thus the vast amount of iodine waste media being stored on nuclear waste treatment facilities internationally can be addressed. Several factors paramount to the successful synthesis of the material will be presented, including the choice of precursors, order of synthesis steps, pH level, and temperature of the solution. Aside from this, solid solutions studies will be presented substituting calcium for lead and phosphate for vanadate. These studies help set a baseline for future apatite compositional studies, so that its characteristics can be optimized for the application of geological repositories with the use of our wet-chemical synthesis method.

Acknowledgement

I would like to thank, first and foremost, my thesis advisor, Prof. Ashutosh Goel. I am forever grateful to you for taking a chance on me and giving me the opportunity to grow and develop as a materials scientist. You have provided me with numerous opportunities over the course of my research that I never would have imagined. You gave me a research topic that I became passionate about and there is no greater feeling than to work on something that you enjoy. I highly appreciate the fact that you believed in me and allowed me the freedom to explore any research ideas and questions that I had. Lastly, I appreciate and cherish the times where we were able to talk and joke, not necessarily about work and research, but just about life in general. Thanks, Professor.

I would also like to thank my committee members, Dr. Dunbar Birnie and Dr. Lisa Klein. Thank you both for being a positive influence during my years as both an undergraduate and graduate student in this department. Dr. Birnie, you were especially welcoming and influential to me as the department chair when I came into the department as an undergrad in 2007 and I thank you for introducing me into this wonderful field of materials science. Dr. Klein, I thank you so much as the graduate director for giving me the opportunity to attend graduate school at Rutgers University. Your guidance and advice along the way has proven invaluable. Thank you!

I would like to thank the U.S. Department of Energy through the Nuclear Energy University Program for sponsoring my research. Without them, none of this would have been possible.

I would like to thank Dr. John McCloy and Saehwa Chong from Washington State University not only for their support in research, but their friendship. Your words of encouragement and support mean a lot to me and I enjoyed the time that we were able to spend together.

I would like to thank the people that have played a huge part in helping me through my years as a graduate student. Bob Horvath, your help is undeniable and I thank you for helping me carry out many of my experiments. I especially appreciate your attention to detail and input when it comes to lab safety. It truly makes a difference in the department. I would like to thank Yaqoot Shaharyar for guiding me, especially during my first few months as a fellow grad student. Your early advice and guidance has been influential over the course of my research. I would like to thank Nahed, Sheela, Claudia, and Michelle. You have all guided me through any administrative questions that I have had and I thank you for making my experience smoother.

I would like to thank my "right-hand man," Taihao Han. Your help as an undergrad in the lab has proven invaluable to me and helped ease the load immensely. I wish you the best of luck in your future endeavors and wish you the best.

I would like to thank my fellow graduate students and postdocs in my research group, Ambar Deshkar, Nick Stone-Weiss, Antoine Brehault, Anne Rebecca, and Prashant Dabas. Your friendship and support means a lot to me. I cherish the fun times that we have had together and promise to keep in touch and wish you all the best in your future endeavors. Thanks, guys!!!

I would like to thank the other undergrads and/or visiting scientists in our research group: Shobhita, Ed, Justin, Yoami, Kim, Nikhil, Steven, Muheez, Ally, Pradeesh, Subhashini, and Hrishikesh. You guys definitely brighten my day as well and I cherish our friendship and wish you the best of luck.

I would like to thank my best friends from Bayonne, New Jersey: Dimitrios Tsakos, Carlos Moran, Hector Lopez, Chris Schubert, and Joe Jimenez. I've known you guys as far back as grade school and I know we got each other's backs for life. Thanks guys for always being there for me. You guys are awesome!

I would like to thank all of the other people that have played a positive role in my career and where I am at today (in no particular order): Mrs. D'Agostino, Mr. Lisk (RIP), Prof. Paul Ellis, Prof. Richard Lehman, Prof. Richard Haber, Prof. Glenn Amatucci, Prof. Frederic Cosandey, Prof. Ahmad Safari, Prof. Adrian Mann, Prof. Richard Riman, Dr. Nathalie Pereira, Dr. Fadwa Badway, Subba Karavadi and all of my fellow IBM friends/co-workers (Adam, Bill, Chris, Larry, Robin, John C, John K, Irene and lastly, John Benedict).

Lastly, I would like to thank my Lord and Savior, Jesus Christ. I know you have a plan for me and without you, none of this would be possible.

Dedication

I dedicate this thesis to my family. You have always been there for me and I love you all. Firstly, I would like to thank my brother, John, and his wife, Christina, and son, Kingsley. John, I love you, bro. As your younger brother, I have always looked up to you and you have no idea how much of a positive influence you have had on me. You have always strived to push me to do my very best and words couldn't describe how much you mean to me. I would also like to thank Christina and little Kingsley for also supporting me and/or brightening my day. Grandma (Katherine Bao Wan), I miss you. It has been a little under a year, since I last saw you, but I know you are in heaven looking down on us. Lastly, I dedicate this to Mom (Lydia) and Dad (Gideon). I love you both and you have been the biggest influences of my life. You pick me up whenever I am down and care for me like no one else could. Whatever I may be going through or whatever decision I make, you are always supporting me. I love you.

Preface

Parts of section 1.3 and the entirety of section 1.4 are from the conference paper,

C. Cao and A. Goel, Apatite Based Ceramic Waste Forms for Immobilization of Radioactive Iodine, An Overview, Proceed. of WM2016 Conference, 2016.

A majority of the analysis and discussion is pending publication in a scientific journal.

Rietveld refinement data in the Results section was provided by our collaborators in Washington State University, Prof. John McCloy and his graduate student, Saehwa Chong.

ICP-MS data in the Results section was provided by collaborators in Corning Inc., Dr. John Mauro and Lynn Thirion

Table of Contents

List of Tables

List of Figures

1. Introduction

Nuclear energy continues to be a reliable contributor to the overall energy production in the United States (and internationally). According to data provided in the November 2016 Monthly Energy Review supplied by the U.S. Energy Information Administration, the percentage of total domestic energy production attributed to nuclear, as opposed to fossil fuel energy production or renewable energy production, amounted to about 9.47% for the year of 2015. Fossil fuels, on the other hand, remained significantly ahead amounting to 79.66%, while renewable energy provided 10.87% of the total energy production supplied domestically.[1] One of the main criticisms of nuclear energy, however, is and always will be the topic of nuclear waste. Due to its radioactivity and harmfulness to the biosphere along with the long half-lives of many of its components, nuclear waste poses a problem in terms of management and disposal. Along with legacy nuclear waste from weapons research and production, a backlog of nuclear waste continues to grow without an actual solution for disposal of most of the waste. Currently, there are vast amounts of nuclear waste collecting at operational nuclear waste treatment facilities around the world.

One consensus path for the disposal of long-lived nuclear waste is the deposition of the waste into a deep geological repository, such as a mountain or salt basin. Currently, only the Waste Isolation Pilot Plant in Carlsbad, New Mexico is functional in the United States and it is only accepting transuranic radioactive waste. Due to political reasons, the Yucca Mountain Project in Nevada was closed in 2011 due to exhausting of federal funding before it was ready to accept any nuclear waste. Regardless of the political climate and availability of geological repositories, however, current nuclear waste still needs to be converted to a waste form that is stable and chemically-durable enough to resist reacting with its environment or degrading over extended

periods of time when deposited into a geological repository. One common example of a stable waste form includes the vitrification of nuclear waste into a borosilicate glass. The research that is being presented in this thesis specifically addresses synthesizing a chemically-durable waste form for the radioisotope, Iodine-129 (referred to as ^{129}I). It will be evident that the immobilization of Iodine poses some very unique challenges that will be addressed.

1.1 Iodine-129

Of the fission products that occur as a result of ^{235}U slow neutron fission, iodine isotopes make up about 0.69% of the overall composition. This translates to about 360 grams of iodine per metric ton of ^{235}U.[2] After two years when the highly radioactive yet short-lived ^{131}I has diminished its dosage to negligible levels, the primary isotopes that remain in the waste are stable ^{127}I and radioactive ^{129}I, which has low-activity, but a substantially long half-life (1.6×10^7 y).[2] Because of this extended half-life duration and the ability of iodine to be highly water-soluble and mobile, ^{129}I waste proves to be a significant challenge in regards to meeting environmental standards and specifications for disposal into a geological repository. In the United Kingdom and France, for instance, the solution to radioactive iodine fission product disposal is to discharge it directly into the sea.[3] The justification is that the dilution of ^{129}I into the vast amount of naturally-occurring ^{127}I isotopes in the sea would minimize the risk of ^{129}I exposure. Considering future changes in regulatory practices, however, it will become necessary to review this strategy and develop waste forms for the immobilization of ^{129}I. U.S regulations, for instance, already require the capture and storage of ^{129}I waste streams for future immobilization into a proper waste form.

One major challenge in developing waste forms for the immobilization of radioactive iodine is that it is not amenable to conventional borosilicate vitrification routes because of its low

solubility in silicate glass chemistries.[4] More importantly, it exhibits high volatility (≥500 °C) at typical glass processing temperatures (1000–1100 °C). Therefore, considerable effort is being made to develop alternative waste forms for iodine immobilization.[5-10] Most proposed waste forms to date, however, have not achieved sufficient maturity and satisfactory properties (specifically: ease of processing, high waste loading, and high chemical durability) to be considered as promising technologies.[2, 11]

1.2 Iodine-129 Waste Management

Over the course of aqueous reprocessing of used nuclear fuel (UNF), the vast majority of iodine waste is converted into an off-gas stream along the different processing steps. That iodine off-gas must then be captured by the waste system in order for it to be stored in some medium. Iodine capture technologies generally fall into two main categories: wet scrubbing and solid sorbents. In wet scrubbing, the off-gas is bubbled through a liquid chemical media, thereby, capturing much of the iodine species in solution. One wet scrubbing technology that is extensively utilized in the United States, as well as many other international reprocessing facilities, is the use of caustic solution (i.e. 1-2 M NaOH). The use of this solution is generally based around the disproportion reaction in Equation 1.

$$3\ I_2\ (g) + 6OH^-\ (aq) \rightarrow 5\ I^-\ (aq) + IO_3^-\ (aq) + 3\ H_2O\ (l) \qquad (1)$$

After this solution is loaded with iodine species, it is either discharged into the sea (i.e. UK or France) or stored in a facility awaiting a future solution to the immobilization of iodine.

Many times in conjunction with caustic scrubbing, solid sorbents are utilized for the capture of iodine in off-gas waste streams. In this technique, the off-gas is flowed through a bed of the solid sorbent, thereby, capturing the iodine due to a chemical reaction. The most common solid sorbents are silver-based and include materials such as silver zeolites, silver nitrate-impregnated alumina, and silver-functionalized silica aerogels. Examples of reactions where silver-based solid sorbents are utilized to capture I_2 (g) or CH_3I (g) to form a solid AgI are presented in Equations 2-5[2].

$$3I_2\ (g) + 6AgNO_3 \rightarrow 4AgI\ (s) + 2AgIO_3\ (s) + 6NO_2\ (g) \quad (2)$$

$$CH_3I\ (g) + AgNO_3\ (s) \rightarrow CH_3NO_3\ (g) + AgI\ (s) \quad (3)$$

$$I_2\ (g) + 2Ag\ (s) \rightarrow 2AgI\ (s) \quad (4)$$

$$2CH_3I\ (g) + 2H_2O\ (g) + 2AgI\ (s) \rightarrow 2AgI\ (s) + 2CH_3OH\ (g) + H_2\ (g) \quad (5)$$

As the same with the liquid caustic solution waste, the solid sorbent waste is stored on the premises of waste processing facilities, awaiting a future solution for immobilization.

1.3 Apatite Mineral

Apatites (general formula, $A_{10}(BO_4)_6X_2$; A and B are cations, X is an anion) are minerals that are best known for their characteristic channel-like crystal structure that extend down the crystallographic c-direction, as shown by Figure 1. The most common apatites exhibit a hexagonal crystal structure with a crystal symmetry of $P6_3/m$. Each cation and anion have their own specific site locations within an apatite with the A-site cations subdivided into two specific locations, often referred to as A(1) and A(2). A(1) cations are typically known for their “column” configuration as they are always directly stacked on top of each other in the c-direction in the crystal structure.

They also can be defined as the connecting cation between characteristic apatite channels and play a significant role in the formation of the walls of the apatite channels. A(2) cations, on the other hand, typically occur as sets of 3 cations in a triangular configuration on each crystallographic plane parallel to the a-direction. Each plane of A(2) triangular units are offset from the plane above and below, so that the best packing fraction is achieved. Due to their configuration, A(2) cations essentially line the interior of the characteristic apatite channels and play a significant role in the accommodation of halide ions in the crystal structure. In terms of the B-site cations, they typically occur as tetrahedral units with oxygen and one of their corners are always pointed towards the interior of an apatite channel, thus also playing a crucial role in the formation of the walls of the apatite channel.

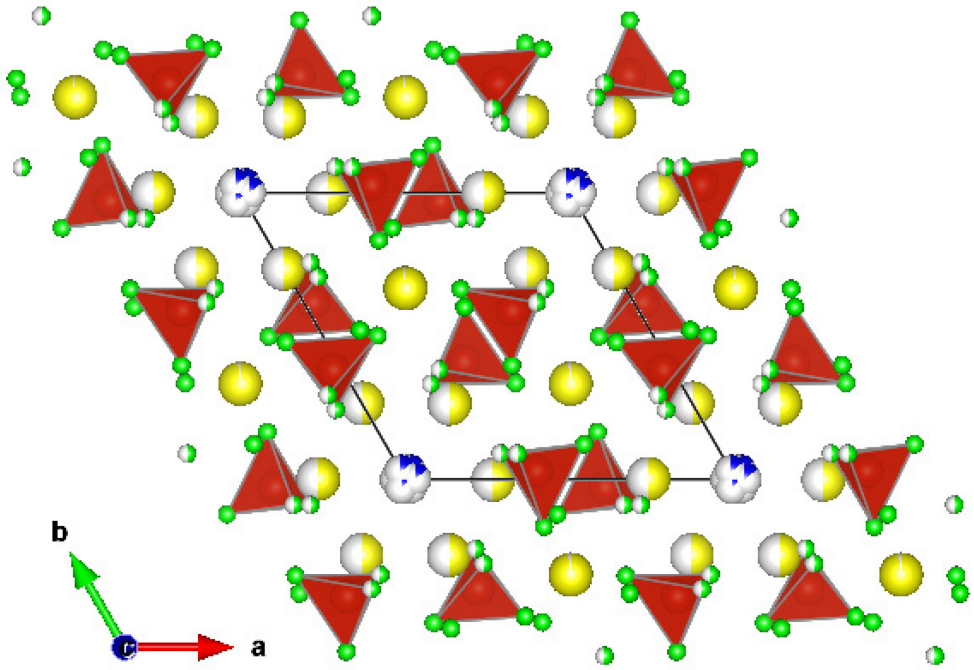

Figure 1. Schematic of the crystal structure of a common apatite structure with $P6_3/m$ symmetry

The X-anion sits in the center of the characteristic apatite channel, oftentimes between the A(2) planes, depending on the size of the anion and they are often the most investigated structural aspect of apatites, given that the incorporation of halide ions often determines the primary characteristics of the apatite. In dentistry, for instance, the use of fluoride helps facilitate the replacement of hydroxyapatite, $Ca_{10}(PO_4)_6(OH)_2$ (which makes up the tooth enamel) with fluorapatite, $Ca_{10}(PO_4)_6F_2$. Given that fluorapatite is more resistant to tooth decay, teeth are made much stronger. This is possible because fluoride ions have a higher affinity for the apatite channel than the hydroxyl ions due to their small ionic radii (and quite possibly also their orbital configuration). Fluoride ions are able to be situated exactly between the A(2) triangular planes, whereas hydroxyl ions are situated just slightly out of plane. In calcium phosphate apatites, the larger the halide the further the anion sits away from the plane. Interestingly enough, in lead phosphate apatites this size trend does not matter as all halides from fluorine to bromine sit at z = ½ (exactly halfway between triangular planes planes). This was hypothesized to be a result of the stereochemical activity of the lead 6s electrons.[13]

Apatites have been long considered as one of the most promising candidate waste forms for the immobilization of radioactive iodine.[6, 14, 15] This is primarily due to their unique channel structure that allows the halide ions to be incorporated into their crystal structure[16], their good chemical durability[11], and their high radiation stability[17, 18]. Experimentally, the majority of investigated apatites can accommodate F^-, Cl^-, Br^-, O_2^-, OH^- and/or CO_3^{2-} in their X-anion site. The choice of apatite minerals where the X-anion site in the structural channel is occupied by I- or IO_3-, however, are highly limited due to the large size of iodide/iodate ions. Considering the large ionic radius of iodide (I^-, 1.96 Å), it is difficult to find any naturally existing iodine-containing apatites, thus leading to a scarce amount of knowledge and basic understanding about iodo-apatites.[12] Due

to these reasons, most of the iodine-containing apatites produced so far have had several shortcomings that have not allowed them to be adopted for iodine immobilization. The shortcomings may be issues, such as low waste (iodine) loading, poor chemical durability, or inability to scale up production. Progress is being made in the development of apatites for iodine immobilization, but in order to find the solution to the problem, one must thoroughly investigate the problem and understand the work that has led to the current state of apatite research within the scientific community.

1.4 Iodo-Apatite Compositions

1.4.1 Early Iodo-Apatites

Early on, iodine-containing apatites were synthesized by various researchers for various purposes. None of those, however, aimed at developing a waste form for immobilization of radioactive iodine. It began as early as 1959 when Merker and Wondratschek were studying lead apatites.[19] It was not, until about four decades later, however, when the topic of iodine immobilization in apatites was brought to light by Audubert et al.[20] Within that timeframe, there were only a few other investigations into iodo-apatites. Sudarsanan et al. synthesized cadmium vanadate iodide apatite from the melt of cadmium vanadate and cadmium iodide.[21, 22] It was concluded that due to a short c-dimension, there were deficiencies in the halide content and, as a result, modifications in the typical apatite structure occurred. This led to the formation of vacancies in the Cd(2) position (which formulates the apatite channel) in order to maintain charge balance. Apart from that, the only other iodo-apatite studies that were reported in this timeframe involved the use of pyramidal perrhenates (ReO_5).[23, 24] This is a step away from the standard structural and chemical moieties, which comprise of a tetrahedral MO_4 structure. For example, Baud et al. made an attempt to synthesize barium perrhenate iodide ($Ba_{10}(ReO_5)_6I_2$) *via* solid state route.[23] However, the as synthesized apatite mineral had the composition $Ba_{10}(ReO_5)_6I_{0.77}(OH)_{1.23}$,

depicting uptake of moisture during synthesis. It was concluded that due to the electrostatic repulsion of the oxygen atoms of the pyramidal perrhenates on the IBa_6 octahedra that hydroxyl ions began to substitute for the halogen within the channel. In another study, Schriewer and Jeitschko, made an attempt to synthesize strontium perrhenate iodide apatite ($Sr_{10}(ReO_5)_6I_2$) *via* solid state route.[24] Although we could not find any information about the experimental chemical composition of the apatite formed in this study, it is interesting to note that the as synthesized iodo-apatite had an orthorhombic crystal structure, whereas the majority of iodo-apatites have hexagonal crystal structure.

1.4.2 Calcium-Phosphate Iodo-Apatites

One of the most commonly-known apatites within the scientific community is hydroxyapatite, which has a chemical formula, $Ca_{10}(PO_4)_6(OH)_2$. Owing to the ability of hydroxyapatite to accommodate halide ions (F^-, Cl^-, Br^-) in its crystal structure, attempts have also been made to incorporate iodide (I^-) for the hydroxyl (OH^-) ion within the apatite channel. However, success in this direction is still eluding the scientists. The only study that has reported on successful substitution of $I^- \leftrightarrow OH^-$ in $Ca_{10}(PO_4)_6(OH)_2$ using wet chemical synthesis has been published by Phebe and Narasaraju.[25] However, their assertions were highly preliminary in nature and it has been difficult to reproduce those results by any other researcher worldwide.[26] The successful attempts to incorporate iodine into calcium phosphate apatites utilized iodate (IO_3^-) instead of iodide (I^-) as the precursor for iodine, resulting in a solid solution with the general formula, $Ca_{10}(PO_4)_6(OH)_{2-x}(IO_3)_x$. The first successful attempt was made by Henning et al. where they synthesized a superstructure of an apatite material with the chemical formula, $Ca_{15}(PO_4)_9IO_3$ using a flux method.[27] However, considering that the material was synthesized at high temperature (850 °C) and under highly controlled conditions, it was difficult to consider this

technique for waste form development. Recently, Campayo et al. synthesized a calcium phosphate iodate apatite with experimental composition $Ca_{10}(PO_4)_6(OH)_{1.6}(IO_3)_{0.4}$ using low temperature wet chemical synthesis aimed at immobilizing iodine.[6] Although halide containing apatites (for example, fluorapatite) are known for their high chemical durability in neutral and basic environments, the structural analysis of iodate-containing hydroxyapatite revealed the lack of local order around the iodate ions as these ions do not cluster around the apatite channels, something that is not typically observed in apatites.[7] This raises concerns about the long term chemical durability of this waste form. Increasing iodine waste loading in these apatites is another crucial aspect that needs to be addressed in the near future.

1.4.3 Lead-Vanadate Iodo-Apatites

Lead-vanadate apatite [$Pb_{10}(VO_4)_6I_2$] has been extensively studied as a potential waste form for iodine immobilization. Due to the fact that lead and vanadium have larger ionic radii than calcium and phosphorous, lead-vanadate apatites are capable of incorporating iodine into its structure. Due to this, many variations on the synthesis of lead-vanadate iodide apatite have been explored over the years. Lead vanadate iodide was first synthesized by Merker and Wondratscheck by melting lead vanadate and lead iodide in a vacuum sealed vessel in the temperature range of 500-800°C, while the crystallographic data on these minerals was obtained by Audubert et al.[19, 28] Further, Audubert et al. synthesized lead vanadate iodide, $Pb_{10}(VO_4)_6I_2$ within a matrix *via* solid state sintering by compacting a lead iodide core within the center of an outer layer of lead vanadate and consolidating the green body at 700 °C and 25 MPa.[20] Other high temperature synthesis methods include (i) mixing stoichiometric amounts of the precursors (PbO, PbI_2, V_2O_5) corresponding to $Pb_{10}(VO_4)_6I_2$, and heating them in a sealed quartz ampoule at 700 °C

for 5 h under 35 MPa pressure, or (ii) hot isostatic pressing at 700°C for 2 h under the pressure of 200 MPa.[29, 30]

Although various solid state synthesis routes have yielded the desired Pb-V-I apatite, the major drawback with these synthesis routes is the need for a higher processing temperature. Iodine typically volatilizes at a temperature >500 °C and, as a result, the majority of the synthesis techniques investigated so far have been confined to sealed vessels and highly controlled environments. This problem is further aggravated by the poor chemical durability of stoichiometric $Pb_{10}(VO_4)_6I_2$ which demonstrates a leach rate (in pure boiling water) that is two orders of magnitude higher than for silver iodide-embedded glass waste forms.[29] This has resulted in a significant research effort focused on developing low temperature synthesis routes and improving the chemical durability of Pb-V-I based apatites. In this pursuit, it was observed that partial substitution of $(VO_4)^{3-}$ by $(PO_4)^{3-}$ in the apatite structure, resulting in a mineral with chemical composition $Pb_{10}(VO_4)_{4.8}(PO_4)_{1.2}I_2$, not only lowered the densification temperature of the ceramic body from 700 °C to 540°C (25 MPa), but also had a significant increase in the densification of the powder compact, thus increasing its chemical durability (due to a decrease in surface area).[31] This development resulted in a flurry of studies involving synthesis of Pb-V-P-I based apatites using various other techniques including spark plasma sintering,[32, 33] microwave dielectric heating,[34] and high energy ball milling.[35] The research in this direction currently still continues to be explored.

1.4.4 Future Research on Iodine-Containing Apatites

As discussed above, most of the research on iodine immobilization in apatites has focused either on Pb-V-I or Ca-P-I system. However, there are several other systems that have

demonstrated their ability to incorporate iodine in their crystal structure. For instance, cadmium vanadate iodide ($Cd_{10}(VO_4)_6I_2$), barium rhenium perrhenate iodide ($Ba_{10}(ReO_5)_6I_2$) and strontium rhenium perrhenate iodide ($Sr_{10}(ReO_5)_6I_2$), are potential candidate waste forms for iodine immobilization.[21, 23, 24] According to a recent computational study on the structure of iodine containing apatites with general formula $A_5(XO_4)_3I$, the A-site cation is capable of holding either Ag^+, K^+, Sr^{2+}, Pb^{2+}, Ba^{2+} and Cs^+, whereas the X-site cation can hold Mn^{5+}, As^{5+}, Cr^{5+}, V^{5+}, Mo^{5+}, Si^{4+}, Ge^{4+} and Re^{7+} depending on the overall chemistry of the system.[16] Therefore, there is enough scope to design chemically durable apatite based waste forms for immobilization of radioactive iodine.

Another area that needs significant research effort in this field is to develop low temperature synthesis methods where these minerals can be produced under ambient conditions. This will not only lower the overall cost of waste form development, but will also allow the integration of a production scale-up. One such example is aqueous processing (for example, co-precipitation technique or hydrothermal synthesis) which has not been reported for Pb-V-I based apatites so far.

1.5 Research Plan

In this study, the development of a low-temperature synthesis method for iodide-containing apatites will be presented. Specifically, it will focus on utilizing wet-chemical synthesis for the production of lead vanadate iodide apatite, $Pb_{10}(VO_4)_6I_2$. Synthesis experiments and characterization of the synthesis products would be performed to achieve the desired material. Several factors will be discussed regarding the successful synthesis of this material, such as

precursor choice, order of synthesis steps, pH, atmosphere and temperature of solution prior to precipitation.

In addition, due to the successful synthesis of this material by the proposed technique, solid solutions of the aforementioned parent apatite will also be presented. Two series of solid solutions will be investigated. Series-1 will focus on the substitution of calcium for lead in the crystal structure, $Pb_{10-x}Ca_x(VO_4)_6I_2$, where x = 0, 2, 4, 6, 8, 10. The reason for choosing $Pb^{2+}\leftrightarrow Ca^{2+}$ substitution in these apatites is based on the fact that $Pb_{(10-x)}Ca_x(VO_4)_6X_2$ have been reported where X = F, Cl, or Br[12, 36] but $Pb_{(10-x)}Ca_x(VO_4)_6I_2$ have not been reported to the best of our knowledge. Further, the impact of $Pb^{2+}\leftrightarrow Ca^{2+}$ substitution on the properties (primarily chemical durability) of these apatites is still unclear. Series-2 will focus on the substitution of phosphate for vanadate in the crystal structure, $Pb_{10}(VO_4)_{6-y}(PO_4)_yI_2$, where y = 1, 2. As been discussed earlier, the introduction into this parent apatite facilitates the lowering of their sintering temperatures. The aim of our investigation of this series is to exhibit the reproducibility of this lead phospho-vanado iodide apatite utilizing a simple developed method.

2. Experimental

2.1 Apatite Synthesis

The chemistry of precursors plays a crucial role in this synthesis method as all the precursors should exhibit high solubility in water. Accordingly, $Pb(NO_3)_2$ (99.0% min, Alfa Aesar) and Na_3VO_4 (99.9% metals basis, Alfa Aesar) were used as precursors for lead and vanadium ions, respectively. The choice of PbI_2 and NH_4VO_3 as precursors of lead and vanadium will not lead to the formation of desired product.

NaI (99.9% metals basis, Alfa Aesar) was used as a precursor surrogate for radioactive iodine. The choice of NaI was made considering that caustic scrubbing (using ~1-2 M NaOH) is the only liquid scrubbing method that is deployed in most of the reprocessing plants for the capture of gaseous iodine (i.e. Hanford waste treatment plant in Washington State).[2] The resultant solution from this scrubbing contains NaI, $NaIO_3$ and perhaps NaOI.

The chemical precursors used for calcium and phosphate in the synthesis of solid solutions were $Ca(NO_3)_2{\cdot}4H_2O$ (99%, Alfa Aesar) and K_3PO_4 (≥98%, Sigma Aldrich), respectively. K_3PO_4 was chosen as the phosphate precursor over Na_3PO_4 after our preliminary experimental analysis suggested that powders obtained using former had higher crystallinity than those synthesized using latter. The step-by-step synthesis of $Pb_{10}(VO_4)_6I_2$ has been described below.

Step 1. The required amount of $Pb(NO_3)_2$, Na_3VO_4 and NaI in accordance with reaction (6) are weighed and dissolved in deionized water on an individual basis.

$$10Pb(NO_3)_2 + 6Na_3VO_4 + 2NaI \rightarrow Pb_{10}(VO_4)_6I_2 + 20NaNO_3 \quad (6)$$

In our study, 4.968 g $Pb(NO_3)_2$, 1.65546 g Na_3VO_4, and 0.44967 g NaI were dissolved in 300 ml deionized water separately in three different beakers corresponding to 0.1 M solution of $Pb(NO_3)_2$, 0.06 M solution of Na_3VO_4, and 0.02 M solution of NaI. All of the solutions were magnetically stirred for 1 h. The concentration of precursor solutions was kept low to ensure that all the precursors react completely.

Step 2. Mix 0.02 M NaI solution with 0.06 M Na_3VO_4 solution and stir for 1 h.

Step 3. Add 0.1 M $Pb(NO_3)_2$ to 0.02 M NaI + 0.06 M Na_3VO_4 solution obtained from Step 2 in a drop-by-drop manner.

Step 4. Allow the solution from Step 3 to stir for additional 3 h ensuring the thorough formation of precipitates. The obtained precipitates are washed with deionized water and dried overnight at 70 – 80 °C.

The synthesis (including mixing of precursor solutions) was performed at ambient temperature (~30 °C). It was observed that temperatures higher than 45 °C (in particular for the aqueous solution of NaI and Na_3VO_4 prior to the formation of precipitates in Step 3) favored the formation of $Pb_{10}(VO_4)_6(OH)_2$ along with $Pb_{10}(VO_4)_6I_2$ considering that OH^- has a higher affinity (than I^-) to incorporate into an X-anion site of $A_{10}(BO_4)_6X_2$ apatite due to its smaller ionic size.[16] [See Supplementary Results] Further, no acid or base was added to control the pH of the final solution or to precipitate the apatite mineral unlike the methodology used in the synthesis of halide-containing calcium phosphate apatites.[6, 37] The addition of HNO_3 or NaOH (even in small concentrations) to the reaction medium will result in the formation of powders with undesired crystalline phases including, for example, chervetite, $Pb_2V_2O_7$, iodolaurionite, Pb(OH)I, (when HNO_3 is added) or hydroxyvanadinite, $Pb_{10}(VO_4)_6(OH)_2$ (when NaOH is added).

In order to synthesize $Pb_{(10-x)}Ca_x(VO_4)_6I_2$ and $Pb_{10}(VO_4)_{(6-y)}(PO_4)_yI_2$ based solid solutions, the methodology is defined by the chemistry of the apatite. In general, the structure of apatite with general formula $A_{10}(BO_4)_6X_2$ consists of two cations, i.e. A and B, where A-cations individually occupy two functionally different sites within the crystal structure, while B-cations are found as tetrahedral units with oxygen in their specific site. Theoretically, both Pb^{2+} and Ca^{2+} can be substituted at the A-cation sites, while V^{5+} and P^{5+} can be substituted at the B-cation site.[12]

Accordingly, during synthesis of $Pb_{(10-x)}Ca_x(VO_4)_6I_2$ apatites, aqueous solutions of $Pb(NO_3)_2$ and $Ca(NO_3)_2{\cdot}4H_2O$ (A-cation solutions) have to be mixed completely before adding the resultant solution (drop-by-drop) to the aqueous solution of 0.02 M NaI + 0.06 M Na_3VO_4 in Step 3 of the synthesis route described above.

Similarly, during synthesis of $Pb_{10}(VO_4)_{(6-y)}(PO_4)_yI_2$ apatites, aqueous solutions of Na_3VO_4 and K_3PO_4 (B-cation solutions) of desired molarities need to be mixed completely with 0.02 M NaI, prior to the addition of $Pb(NO_3)_2$ in Step 3 of the synthesis route described above. If the precursors are mixed in an incorrect sequence, the solution will prematurely precipitate an undesired mineral and apatite synthesis will no longer be possible.

2.2 Characterization

The qualitative and quantitative crystalline phase analysis of dried powders were performed by X-ray diffraction (XRD; PANalytical X'Pert Pro MPD; Cu-K_α source at 45 keV and 40 mA; 2θ = 10-90° with 0.002° 2θ step size and dwell time of 5.7 s). 5 or 10 wt.% ZnO (NIST SRM-674b) was used as an internal standard. The quantitative phase analysis was performed by Rietveld – Reference Intensity Ratio (RIR) method using PANalytical Highscore software. The structural analysis of powder samples was performed by Raman spectroscopy (Renishaw inVia Raman microscope; 633nm wavelength laser, operating at 10% power; acquisition dwell time = 40 s from the range of 100-1700 cm^{-1} with a 50x objective). X-ray fluorescence (XRF; Epsilon 1, PANalytical B.V.; Ag anode) was used to quantify the elemental composition in powder samples. In order to improve quantification, oxygen was attributed to any potential B-site cations present due to its inability to be detected individually. The iodine concentration in the remnant solution was analyzed by inductively coupled plasma – mass spectroscopy (ICP-MS; PerkinElmer).

3. Results

3.1 Synthesis of $Pb_{10-x}Ca_x(VO_4)_6I_2$ series

Figure 2 presents the XRD data of powder samples from the series, $Pb_{(10-x)}Ca_x(VO_4)_6I_2$, where x varies between 0 – 10. For sample x = 0, the XRD data shows intense phase reflections corresponding to $Pb_{9.85}(VO_4)_6I_{1.7}$ (PDF#97-028-0065) phase, thus confirming the synthesis of lead vanadate iodide (apatite) mineral. The deviation from the ideal stoichiometric formula of $Pb_{10}(VO_4)_6I_2$ is attributed to the presence of stoichiometric deficiencies in the structure as has been explained by Audubert et al.[28] The quantitative crystalline phase analysis of this sample (Table 1) reveals the presence of ~53 wt.% crystallinity in the sample.

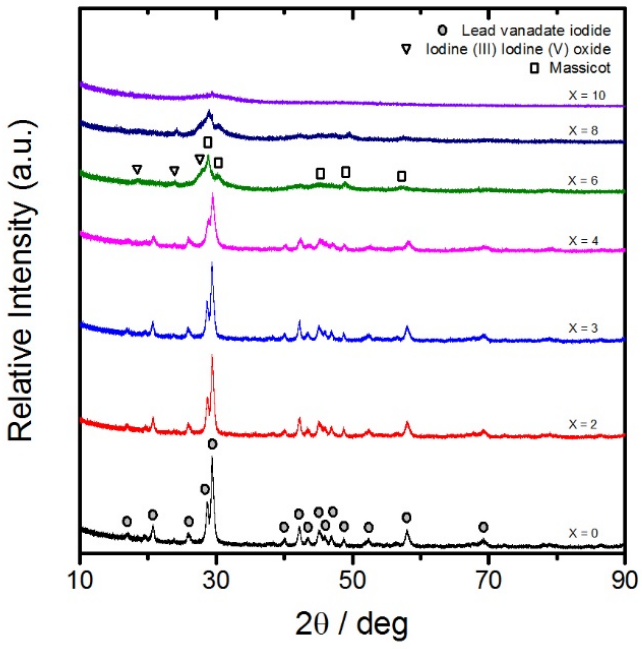

Figure 2. XRD patterns of $Pb_{(10-x)}Ca_x(VO_4)_6I_2$ apatite series (x = 0-10)

		Phase Wt%					
x	Sample Formula	Amorphous	Lead Vanadate Iodide $Pb_{9.85}(VO_4)_6I_{1.7}$	Hydroxyvanadinite $Pb_{9.262}(VO_4)_6(OH)_{1.4}$	Litharge PbO	Massicot PbO	Iodine (III) Iodine (V) Oxide I_2O_4
0	$Pb_{10}(VO_4)_6I_2$	46.8	53.2				
2	$Pb_8Ca_2(VO_4)_6I_2$	50.4	49.5				
3	$Pb_7Ca_3(VO_4)_6I_2$	44.1	50.9	5.0			
4	$Pb_6Ca_4(VO_4)_6I_2$	46.4	41.4	9.8	2.4		
6	$Pb_4Ca_6(VO_4)_6I_2$	78.1	13.9			5.2	2.9
8	$Pb_2Ca_8(VO_4)_6I_2$	83.6	8.9			6.6	0.9
10	$Ca_{10}(VO_4)_6I_2$	100					

Table 1. Rietveld refinement of $Pb_{(10-x)}Ca_x(VO_4)_6I_2$ apatite series (x = 0-10)

The gradual substitution of Ca^{2+} for Pb^{2+} in the theoretical apatite composition of $Pb_{(10-x)}Ca_x(VO_4)_6I_2$ resulted in broadening of XRD peaks. The quantitative crystalline phase analysis of these samples reveals an increase in amorphous content in samples with increasing Ca^{2+}/Pb^{2+} ratio (in particular for x = 6 – 10) with sample x = 10 being completely amorphous (Figure 2). From the viewpoint of the formation of solid solutions, lead vanadate iodide, $Pb_{9.85}(VO_4)_6I_{1.7}$, was the only phase for sample with x = 2. For x = 3, minor amounts (~5 wt.%) of the hydroxyvanadinite ($Pb_{9.262}(VO_4)_6(OH)_{1.4}$; PDF#97-015-5416) apatite phase was observed with $Pb_{9.85}(VO_4)_6I_{1.7}$ still being the dominant phase. Further increase in Ca^{2+}/Pb^{2+} ratio (at x = 4) resulted in crystallization of ~2.4 wt.% litharge (PbO; PDF#97-006-2842; tetragonal) along with lead vanadate iodide and hydroxyvanadinite, with lead vanadate iodide still being the primary crystalline phase (~41 wt.%). For samples x = 6 and 8, the amorphous content in samples significantly increased from 46.4 wt.% (at x = 4) to 78 wt.% (at x = 6) and 83.6 wt.% (at x = 8). While lead vanadate iodide was still the primary crystalline phase in both the samples, massicot (PbO; PDF#97-065-3900; orthorhombic) and I_2O_4 (PDF#97-007-8386) were found in their crystalline phase assemblages in minor concentrations.

XRD data suggests the formation of apatite structure solid solutions in $Pb_{(10-x)}Ca_x(VO_4)_6I_2$ for x = 0 – 3. However, the chemical compositions of the synthesized mineral powders and their

respective remnant reactant solutions, which were analyzed by XRF (Table 2) and ICP-MS (Table 3), respectively, suggest otherwise. The results obtained from chemical analysis of powder samples and reactant solutions are summarized below.

i. The synthesized $Pb_{10}(VO_4)_6I_2$ apatite exhibited an iodine loading of ~9.4 wt.% as deduced by XRF spectroscopy. This is close to the theoretical value of 8.4 wt.% as calculated for stoichiometric $Pb_{10}(VO_4)_6I_2$. The concentration of iodine decreased from 2600 ppm (mg/l) in the precursor solution (0.02 M NaI) to 140 ppm in the remnant reactant solution after synthesis of $Pb_{10}(VO_4)_6I_2$ apatite (as shown in Table 3), thus, demonstrating an uptake of 94.62%.

ii. XRF data reveals that a negligible amount of calcium was incorporated into the apatite crystal structure, thus suggesting that the A-cation sites in the structure were dominantly occupied by Pb^{2+} ions. The as synthesized $Pb_{10}(VO_4)_6I_2$ (x = 0) apatite contained ~990 ppm calcium (Table 2) which may be attributed to impurities present in the precursor materials. For minerals with ideal composition $Pb_{10-x}Ca_x(VO_4)_6I_2$ with x varying between 2 (2.99 wt.%) – 4 (6.83 wt.%), the concentration of calcium in their experimental analogues was found to be constant at ~0.32 wt.%. Further increase in calcium content (x = 6 – 10) in the ideal apatite composition induced high concentrations of amorphous character in their experimental analogues which allowed accommodation of significantly higher amounts of calcium as shown in Table 2. These results were corroborated by ICP-MS analysis of remnant reactant solution where the concentration of Ca^{2+} was found to increase from 0.824 ppm (for x = 0) to 780 ppm (for x = 10) implying that a majority of calcium stayed back in the solution as opposed to being incorporated into the crystal structure.

Intended Sample	Normalized Weight %									
	Th. Pb%	Exp. Pb%	Th. Ca%	Exp. Ca%	Th. VO_4%	Exp. VO_4%	Th. PO_4%	Exp. PO_4%	Th. I%	Exp. I%
$Pb_{10}(VO_4)_6I_2$	68.71	70.3606	0	991ppm	22.87	19.6800	0	0.5210	8.42	9.4384
$Pb_8Ca_2(VO_4)_6I_2$	61.82	70.0900	2.99	0.3183	25.72	19.7768	0	1.0371	9.47	8.7777
$Pb_6Ca_4(VO_4)_6I_2$	52.97	70.5788	6.83	0.3219	29.38	21.3383	0	1.0244	10.81	6.7366
$Pb_4Ca_6(VO_4)_6I_2$	41.18	64.8398	11.95	3.9584	34.26	29.8946	0	1.0115	12.61	0.2957
$Pb_2Ca_8(VO_4)_6I_2$	24.69	50.6042	19.10	11.7761	41.09	36.9168	0	0.7029	15.12	882ppm
$Ca_{10}(VO_4)_6I_2$	0	67ppm	29.81	35.1371	51.30	64.3260	0	0.5369	18.88	808ppm
$Pb_{10}(VO_4)_5(PO_4)I_2$	69.17	71.7276	0	0.3332	19.22	15.6740	3.17	3.8088	8.47	8.4564

Table 2. XRF analysis of select apatites

Sample	pH	Concentrations in mg/L (ppm)						
		Pb	Ca	V	P	I	Na	K
$Pb_{10}(VO_4)_6I_2$	3.53	~2400	0.824	<0.010	<0.050	140	~970	1.41
$Pb_8Ca_2(VO_4)_6I_2$	3.96	~800	~200	<0.010	<0.050	140	~790	1.41
$Pb_6Ca_4(VO_4)_6I_2$	4.80	6.6	~440	<0.010	<0.050	300	~870	1.61
$Pb_4Ca_6(VO_4)_6I_2$	9.10	0.016	~500	13.8	<0.050	530	~800	1.49
$Pb_2Ca_8(VO_4)_6I_2$	9.89	<0.010	~570	~90	<0.050	540	~880	1.63
$Ca_{10}(VO_4)_6I_2$	10.36	<0.010	~780	~120	0.168	670	~1200	2.08
$Pb_{10}(VO_4)_5(PO_4)I_2$	4.01	~1600	0.32	0.015	<0.050	170	~660	286
NaI Reference	6.20	0.013	0.16	<0.010	<0.050	2600	~480	0.605

Table 3. ICP-MS analysis of select apatite synthesis remnant solutions

Since substitution of Ca^{2+} for Pb^{2+} in the $Pb_{(10-x)}Ca_x(VO_4)_6I_2$ series induced high amorphous character in the synthesized minerals, Raman spectroscopy was used to study their structural transformations. Figure 3 presents the Raman spectra of all the as synthesized minerals (x = 0 – 10). The Raman spectra of $Pb_{10}(VO_4)_6I_2$ (x = 0) apatite exhibits a sharp band at 824 cm^{-1} corresponding to v_1 symmetric stretching, followed by a shoulder at 777 cm^{-1} and a small band at ~698 cm^{-1} depicting v_3 antisymmetric stretching of V–O bonds.[30, 38] The multiple bands in the low wavenumber region of 300 – 400 cm^{-1} mainly correspond to v_3 bending vibrations of O–V–O bonds.[30] The band 161 cm^{-1} is presumably attributed to the libration of VO_4 parallel to the c-axis.[38] Similar spectra were observed for minerals with x = 0 – 4, thus, confirming minimal structural changes due to calcium incorporation. A weak band (shoulder) can be observed at 877 cm^{-1} for mineral x = 0 which gradually disappears with increasing calcium concentration from x = 0 – 4. This band was not observed by Zhang et al.[30] in their Raman spectra of $Pb_{10}(VO_4)_6I_2$ apatite. The

band has been attributed to symmetric stretching of VO_3 units in $(HVO_4)^{2-}$ and and $(V_2O_7)^{4-}$ species in aqueous vanadate solutions, as observed by Griffith and Wickins[39], and is hypothesized to be a product of the variances in solution pH among the different compositions .

For x = 6 – 10, noticeable structural transformations occur in the synthesized minerals as is evident from their Raman spectra. The first evident observation was the broadening of Raman bands, which is typical for materials with high amorphous character. The bands at 830 cm^{-1} and 839 cm^{-1} corresponding to v_1 symmetric stretching of V–O bonds in apatite structure were still the most intense structural features in minerals with x = 6 and 8, respectively, thus, corroborating the quantitative XRD results. The band at 877 cm^{-1} corresponding to symmetric stretching of VO_3 units became highly prominent in the spectra of sample with x = 6 while this band shifted to 897 cm^{-1} for samples x = 8 and 10.[39] Interestingly, the band at 897 cm^{-1} became the most intense band for sample x = 10 while the band corresponding to v_1 symmetric stretching of V–O bonds in apatite structures appeared as a minor feature centered at ~823 cm^{-1}. This implies a dominance of amorphous $(V_2O_7)^{4-}$ structural species in the sample x = 10. This assertion gains support due to the presence of a broad band at ~227 cm^{-1} and an intense band in the region 300 – 400 cm^{-1} in samples with x = 6 – 10 confirming the presence of $(V_2O_7)^{4-}$ units.[39] The presence of amorphous $(V_2O_7)^{4-}$ units in these minerals (x = 6 – 10) is also supported by the fact that the addition of any acid during synthesis has been shown to produce chervetite ($Pb_2V_2O_7$) instead of apatite (as reported in the experimental section of the paper). Therefore, it is highly likely that amorphous $Ca_2V_2O_7$ may have been formed in these minerals due to the deviation from ideal crystalline synthesis conditions and the analogous nature between the two cations, Pb^{2+} and Ca^{2+}.

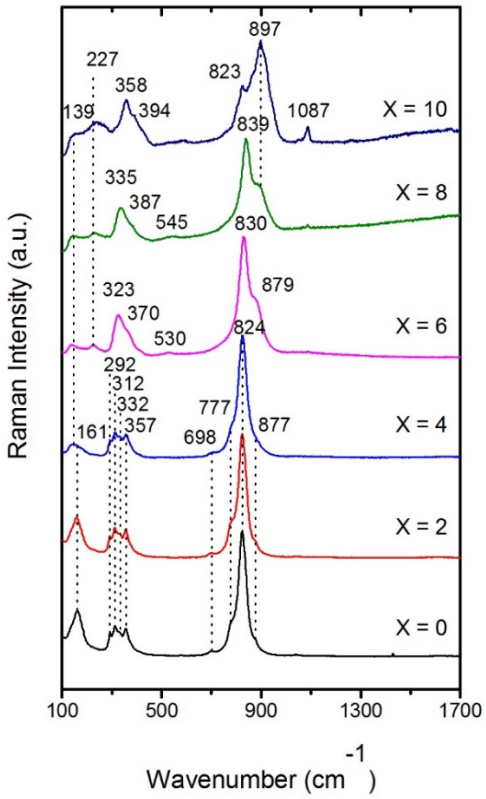

Figure 3. Raman spectra of $Pb_{(10-x)}Ca_x(VO_4)_6I_2$ apatite series (x = 0-10)

3.2 Synthesis of $Pb_{10}(VO_4)_{(6-y)}(PO_4)_yI_2$ series

Figure 4 presents the X-ray diffractograms, while Table 4 presents the quantitative phase analysis of powder samples from the series, $Pb_{10}(VO_4)_{(6-y)}(PO_4)_yI_2$, where y varies between 0-2. The XRD phase analysis of minerals with y>2 has not been presented as $Pb_{10}(VO_4)_{(6-y)}(PO_4)_yI_2$ solid solution did not exist for y ≥2 (as evidenced by the absence of any apatite phases).

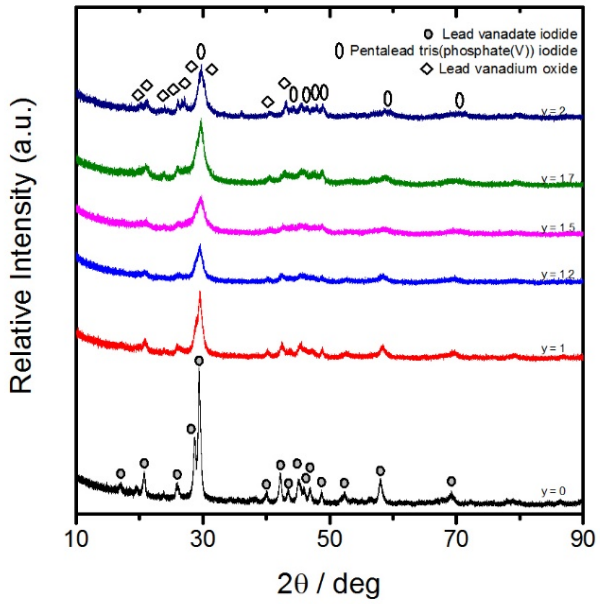

Figure 4. XRD patterns of $Pb_{10}(VO_4)_{(6-y)}(PO_4)_yI_2$ apatite series (y = 0-2)

		Phase Wt %						
y	Sample Formula	Amorphous	Lead Vanadate Iodide $Pb_{9.85}(VO_4)_6I_{1.7}$	Hydroxyvanadinite $Pb_{9.262}(VO_4)_6(OH)_{1.4}$	Litharge PbO	Lead Vanadium Oxide $Pb_{2.667}V_{1.333}O_{5.96}$	Pentalead Tris (phosphate) Iodide $Pb_{10}(PO_4)_6I_2$	Decalead Hexakis Dihydroxide $Pb_{10}(PO_4)_6(OH)_2$
1	$Pb_{10}(VO_4)_5(PO_4)I_2$	40.8	51.2	3.4	4.6			
2	$Pb_{10}(VO_4)_4(PO_4)_2I_2$	30.8				39.5	16.5	13.3

Table 4. Rietveld analysis of $Pb_{10}(VO_4)_{(6-y)}(PO_4)_yI_2$ apatite series (y = 1, 2)

For y = 1, a large percentage of the lead vanadate iodide apatite phase is present along with lower traces of the OH- analogue, hydroxyvanadinite (3.4 wt.%), $Pb_{10}(VO_4)_6(OH)_2$, and a non-apatite phase, litharge (4.6 wt.%), PbO. This suggests the competition for spatial requirements within the apatite structure. As the phosphate content increases, the peaks become much broader. However, unlike $Ca^{2+}\leftrightarrow Pb^{2+}$ substitutions, the XRF and ICP-MS data supports the formation of solid solutions for the partial substitution of $(VO_4)\leftrightarrow(PO_4)$ as summarized below.

i. When y = 1, the experimental weight percent of phosphate within the synthesized apatite mineral was obtained to be 3.8 wt.%, as seen in the XRF data in Table 2. This is in good

agreement with the theoretical concentration (3.17 wt.%) of phosphate ions present in the mineral.

ii. The compositional analysis of the remnant reactant solution supports the hypothesis of solid solution formation as seen in the ICP-MS data present in Table 3. When y = 1, the concentration of phosphate ions remains at a low level in reference to the base apatite, $Pb_{10}(VO_4)_6I_2$. This is opposite to the observations made in the $Pb_{(10-x)}Ca_x(VO_4)_6I_2$ series where the calcium concentration in remnant solutions was found to increase with increasing the value of x. This further suggests that the phosphate ions are incorporated into the apatite crystal structure.

As is evident from XRD data (Table 4), a solid solution does not exist at y = 2. A combination of amorphous content and several crystalline phases, such as lead vanadium oxide ($Pb_{2.667}V_{1.333}O_{5.96}$), pentalead tris(phosphate) iodide ($Pb_{10}(PO_4)_6I_2$), and decalead hexakis dihydroxide ($Pb_{10}(PO_4)_6(OH)_2$) were observed. Therefore, several apatite syntheses were performed with values of y varying between 1 – 2 in order to find the limit of substitution of phosphate for vanadate ions in the apatite structure. The threshold limit of $(PO_4)\leftrightarrow(VO_4)$ substitution in $Pb_{10}(VO_4)_{(6-y)}(PO_4)_yI_2$ was found to be y = 1.5 (8.33 mol.% or 4.77 wt.%). Non-apatitic phases were observed in mineral with y = 1.7.

4. Discussion

The crystal structure of an apatite ($A_{10}(BO_4)_6X_2$) with $P6_3/m$ symmetry is comprised of A- and B- cation sites occupied by Pb and V, respectively, in $Pb_{10}(VO_4)_6I_2$, while the iodide ion occupies the X – anion site, as shown in Figure 5. The A-cation is further divided into two different configurations: A(1) and A(2). The column configuration of A(1) cations along with their

interaction with tetrahedral units composed of B-cations form the walls of the characteristic apatite channel which extends along the crystallographic c-direction. The A(2) cations line the inside of the apatite channel and play a major role in the interaction of the intended X-anion with the apatite.

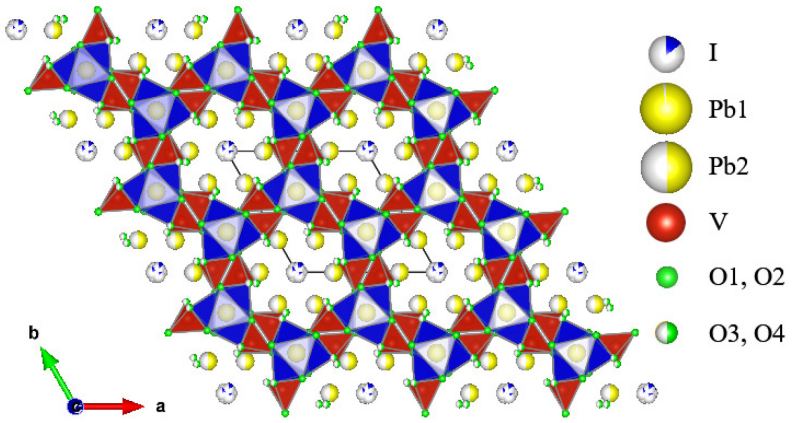

Figure 5. Structural schematic of $Pb_{9.85}(VO_4)_6I_{1.7}$

In order for the iodide to be incorporated into the structural channel, the channel size has to be compatible with the size of the ion. Therefore, the ionic and crystal radii of cations (A and B, respectively), based off of the proper charge and coordination number (CN), play a critical role in deciding the fate of anion incorporation in the apatite structure. The $Pb_{10}(VO_4)_6I_2$ apatite has the relatively large Pb^{2+} ion (ionic radii: 1.19 Å, CN=6)[40] in the A(1)/A(2) sites and VO_4 in the tetrahedron site, leading to a large channel size.[20] For this reason, it is possible to synthesize $Pb_{10}(VO_4)_6I_2$ apatite. However, substitution of a smaller ion, i.e. Ca^{2+} (ionic radii: 1.00 Å, CN=6)[40], for Pb^{2+} reduces the channel size, thus not allowing the large iodide ion to be incorporated into the apatite structure. Similar reasoning can be provided for the substitution of the phosphorus ion (P^{5+}; crystal radii: 0.31 Å, CN=4)[40] for the vanadium ion (V^{5+}; crystal radii: 0.495 Å, CN=4)[40] at the B-cation site, which eventually results in narrowing of the channel size. Therefore, only partial substitutions of Ca^{2+} for Pb^{2+}, and P^{5+} for V^{5+} are possible in the $Pb_{10}(VO_4)_6I_2$ apatite systems.

In our study, the investigation of calcium substitution helps to establish a baseline of compatible cations capable of forming iodine-containing solid solutions by wet chemical precipitation. When paired with molecular modeling, a comprehensive understanding of the structural consequences of substitution can be properly grasped. In a recent study by Wang[16], for instance, an artificial neural network (ANN) approach was utilized to predict candidate cations for the synthesis of appropriate apatite compositions that are capable of incorporating iodine. The results reported in our work show very good correlation with the computational study of Wang.[16]

By utilizing the experimental XRF data and defining the maximum wt.% of Ca that the base apatite, $Pb_{10}(VO_4)_6I_2$, can accommodate as a solid solution as 0.32% (as evidenced by x = 2, 4; Table 2) and considering the summation of A-site cations (Pb+Ca) to be equal to 10, we can calculate a theoretical chemical formula resulting in a $Pb_{9.76}Ca_{0.24}(VO_4)_6I_2$ solid solution. Using a weighted average of the ionic radii of Pb (1.19Å, 2+, CN=6) and Ca (1.00Å, 2+, CN=6) calculated according to the estimated formula, the average radii of A-cations (Pb, Ca) is 1.185Å. When correlated with the crystal radii of vanadium (0.495Å, 5+, CN=4), the resultant estimated channel size agrees very closely with the threshold of iodine accommodation as proposed by Wang.[16]

By applying the same methodology through reverse calculations, an ideal chemical formula for a complete iodine-containing apatite solid solution can be determined as well. In the synthesis of lead vanadate-phosphate solid solutions, by utilizing the ionic radii of lead (1.19Å) in conjunction with the modelled apatite channel size threshold, the average crystal radii of the B-cation can be estimated to be approximately 0.475Å. By using a weighted average for the B-cations and considering the summation of B-site cations (V+P) to be equal to 6, the predicted

chemical formula for the iodine-containing solid solution is $Pb_{10}(VO_4)_{5.35}(PO_4)_{0.65}I_2$. In comparison to the acquired experimental phosphate wt.% of 3.8 (when y=1) with the ideal calculated phosphate wt.% of 2.056 of this formula, the model proves again its utilization as a possible tool for apatite composition determination.

By determining a room temperature method to synthesize Pb-V-I based iodoapatites by wet-chemical precipitation, a viable path towards efficient immobilization of iodine radioisotopes has been created. Due to the minimization of steps required to synthesize iodoapatites under ambient conditions, synthesis of iodine waste forms on a large scale becomes much more feasible in comparison to the other high temperature or multi-step synthesis routes reported in the literature. In addition, the aqueous-based synthesis of solid solutions allows for the investigation of alternative apatite compositions to the well-known lead vanadate iodide to be explored with much more ease, thereby hopefully optimizing the chemical characteristics to the ideal chemical durability and compatibility with geological repositories. The possibility of mixed halide incorporation would additionally serve as a possible benefit given the nature of the apatite mineral.

5. Conclusion

$Pb_{10}(VO_4)_6I_2$ apatite waste forms have been synthesized by one pot wet chemical synthesis at room temperature. The iodine waste loading of the synthesized waste form has been shown to be 9.4 wt.%, while its loading efficiency has been experimentally calculated to be 94.62%. Furthermore, it was found that calcium has minimal tendency to form apatite solid solution when substituted for lead. It tends to form amorphous $Ca_2V_2O_7$ instead. On the other hand, phosphate forms a solid solution with $Pb_{10}(VO_4)_6I_2$ when partially substituted for vanadate ion. The threshold

solubility limit of (PO_4) has been found to be 4.77 wt.%. The chemical durability and sintering behavior of the developed waste forms will be discussed in future studies.

6. Future Work

6.1 Glass Binder Studies

Given that lead vanadate iodide-based apatites exhibit reasonable leach resistance characteristics, yet still fail to satisfy the strict regulations required for disposal into a deep geological repository[30], an alternative strategy to the consolidation of the apatite powder is necessary to improve the chemical durability. Inspired by work by Donald et al. in which ceramic particulates of chlorapatite, $Ca_{10}(PO_4)_6Cl_2$, and spodiosite, $Ca_2(PO_4)Cl$, were encapsulated by a B_2O_3 modified sodium aluminum phosphate glass through sintering for the purpose of chloride waste immobilization, investigations into a glass binder compatible with the currently investigated lead vanadate iodide apatite were conducted.

It was determined that a P_2O_5 – PbO – V_2O_5 ternary system would be most suitable for this application, given that its thermal characteristics satisfied the proper conditions that were desired. Consolidation and sintering were to be investigated at temperatures of 400 °C and 425 °C and, therefore, glasses with glass transition temperatures slightly below these temperatures were desired. Additionally, a focus on avoiding glass crystallization would be necessary given that crystallization would have a negative influence on the chemical durability of the glass-ceramic composite. In addition, the usage of a Pb – P – V system on an apatite capable of utilizing the same components hopefully helps to minimize the experimental variables and potential undesired crystalline phases.

Two series of glasses have already been synthesized in our investigation. Series-1 maintains a constant 30 mol% P_2O_5, while varying the percentages of the PbO and V_2O_5 components. Series-2, on the other hand, maintains a constant 40 mol% PbO, while varying the percentages of P_2O_5 and V_2O_5. A ternary diagram is presented in Figure 6 and preliminary thermal characterization data is presented in Table 5.

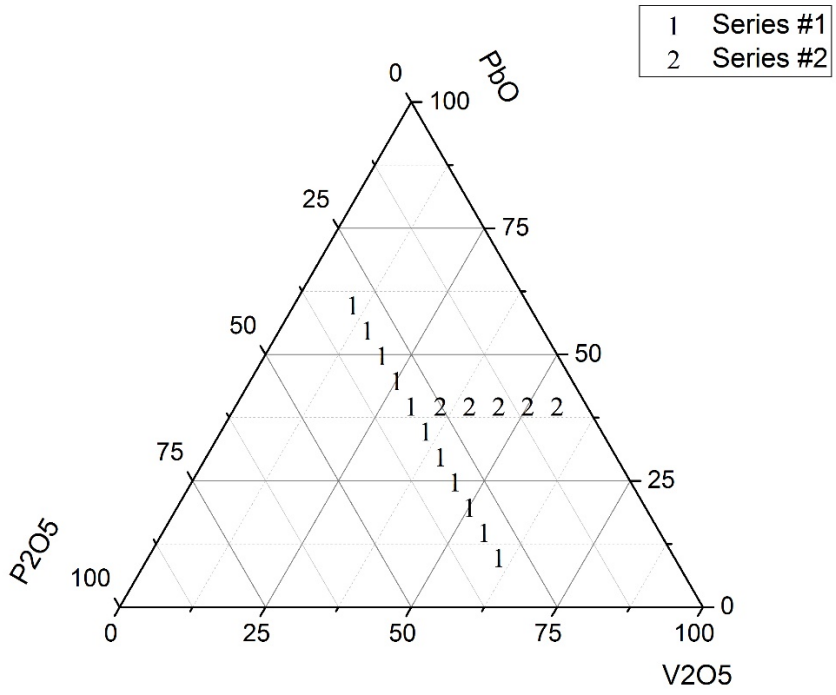

Figure 6. Ternary diagram of proposed P-Pb-V glass series

Series #	Mol % P_2O_5	PbO	V_2O_5	T_g (°C)
1	30	10	60	320.21
	30	15	55	328.38
	30	20	50	333.09
	30	25	45	347.95
	30	30	40	355.11
	30	35	35	360.76
	30	40	30	371.24
	30	45	25	377.04
	30	50	20	386.31
	30	55	15	392.22
	30	60	10	396.28
2	25	40	35	333.74
	20	40	40	304.25
	15	40	45	283.40
	10	40	50	267.87
	5	40	55	250.44

Table 5. Glass transition temperatures (inflection) of proposed P-Pb-V glass compositions

6.2 Silver Iodide – Sodium Iodide Conversion

As mentioned in section 1.2, there are generally two popular techniques utilized for the capture of iodine off-gas during the reprocessing of used nuclear fuel: caustic scrubbing and silver solid sorbents. Given that the aforementioned research thesis focuses on an aqueous synthesis method for producing iodide-containing apatites, there is the question of addressing the silver solid sorbent media and how to convert that capture media into a waste form.

When iodine off-gas comes into contact with the silver solid sorbent, AgI is formed locally within the structure of that sorbent. Currently, however, there is limited literature on the conversion of AgI into NaI, which would be necessary in order to convert AgI eventually into an

iodo-apatite waste form. From our preliminary experiments, it has been determined that this conversion is possible through the use of Na_2S, according to reaction (7).

$$2AgI\ (s) + Na_2S\ (aq) \rightarrow Ag_2S\ (s) + NaI\ (aq) \quad (7)$$

Prior to proceeding with the experiment, there were several factors that needed to be considered. One primary factor was the atmosphere of the reaction vessel. According to the Merck Index, aqueous solutions of sodium sulfide upon exposure to air slowly converts to sodium hydroxide and sodium thiosulfate, according to reaction 10.[41]

$$2Na_2S\ (aq) + 2O_2\ (g) + H_2O\ (l) \rightarrow Na_2S_2O_3\ (aq) + 2NaOH\ (aq) \quad (8)$$

By altering the pH and/or the species present in the solution, the reaction of the intended species may be altered. Another factor that needed to be considered was the photosensitivity of the AgI precursor to be converted. Silver halides are very photosensitive and, therefore, the question was whether the conversion of ionic silver iodide to traces of metallic silver iodide make a difference in the conversion of AgI into NaI. Typically, it would be presumed that the silver solid sorbent in usage would be contained in some opaque containment vessel, but the question of whether precautions for light needing to be considered was a viable question. Lastly, the hygroscopicity and appropriate species of Na_2S precursor needed to be considered, at least in a small lab setting. Given that Na_2S is highly hygroscopic, the absorption of water from the ambient air environment can introduce experimental error and affect the stoichiometry of the reaction.

With all of these considered, the following procedure was followed.

Step 1. The species of Na_2S was verified by x-ray diffraction. (The purchased anhydrous Na_2S had converted to $Na_2S \cdot 5H_2O$ at the time of iteration of the successful experiment).

Step 2. Dissolve the appropriate stoichiometric amount of $Na_2S \cdot 5H_2O$ into deionized water under an argon atmosphere using a 3-neck flask and allow to stir for 30 minutes.

Step 3. Deposit the appropriate stoichiometric amount of deliberately-exposed AgI into the aqueous $Na_2S \cdot 5H_2O$ solution and allow to stir for one hour.

Following filtering and drying, the XRD pattern shown in Figure 7 exhibits complete conversion of AgI into a black precipitate of Ag_2S, thereby leaving NaI in solution. With the use of this exact solution, lead vanadate iodide apatite was reproduced, as seen in the XRD pattern in Figure 8.

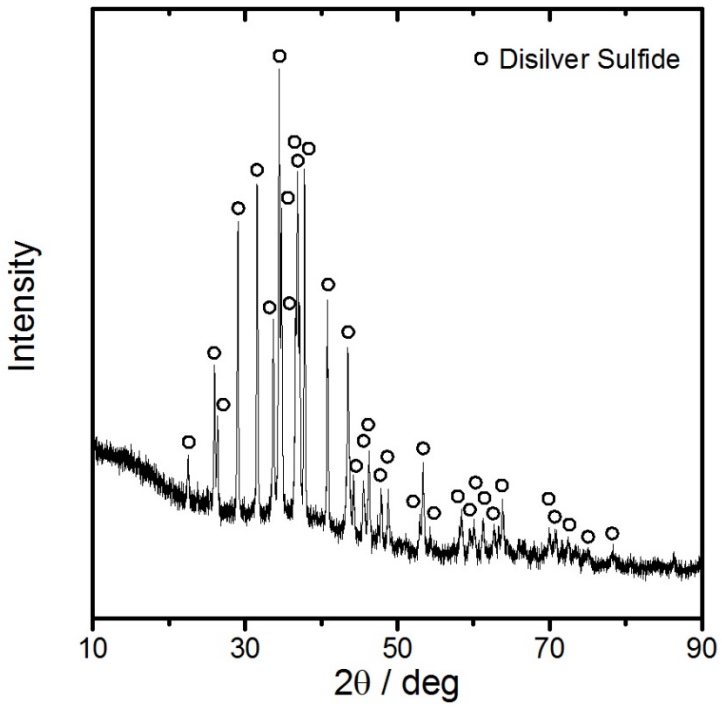

Figure 7. XRD pattern of Ag_2S, suggesting complete conversion of AgI

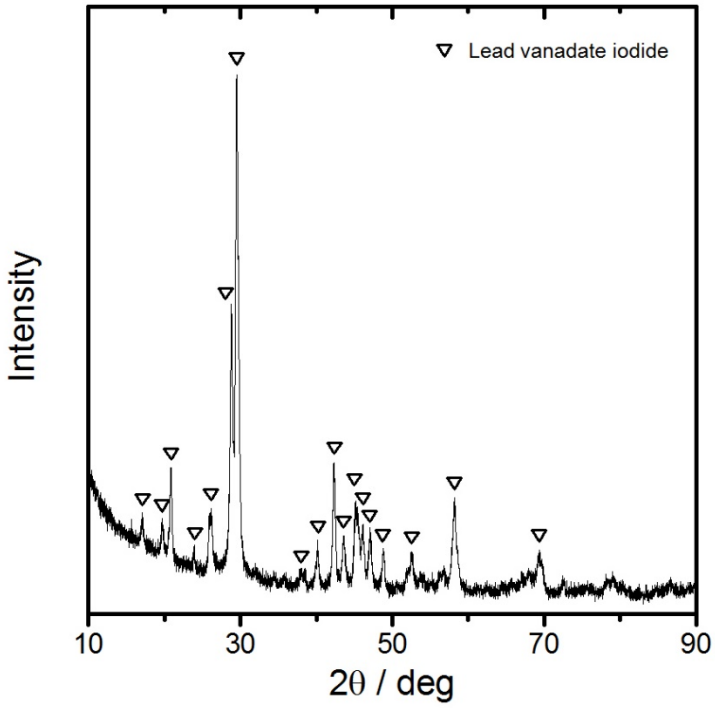

Figure 8. XRD pattern of lead vanadate iodide apatite, synthesized with the remnant solution of AgI-NaI conversion

Further experiments need to be performed in order to determine whether the experimental precautions were actually necessary, including mainly the control of the atmosphere and the photosensitivity of AgI. Regardless, it is evident that through our research solid iodine waste and liquid iodine are both being addressed.

7. Supplementary Results

7.1. Temperature Influence on Apatite Synthesis (in relation to section 2.1)

As seen in Figure 9, the influence of temperature on the synthesis of lead vanadate iodide apatite by wet-chemical synthesis is very important. If the temperature of the VO_4/I solution is heated above 45 °C prior to the addition of $Pb(NO_3)_2$ and the precipitation of the apatite, XRD

peaks attributed to hydroxyvanadinite, $Pb_{10}(VO_4)_6(OH)_2$, the hydroxyl-analogue of the lead vanadate apatite, is exhibited. This is hypothesized to be a result of the deprotonation of water molecules as the water is being heated. If hydroxyl ions are taking the X-anion location within the characteristic apatite channel, the loading of iodide ions in the apatite should be greatly affected.

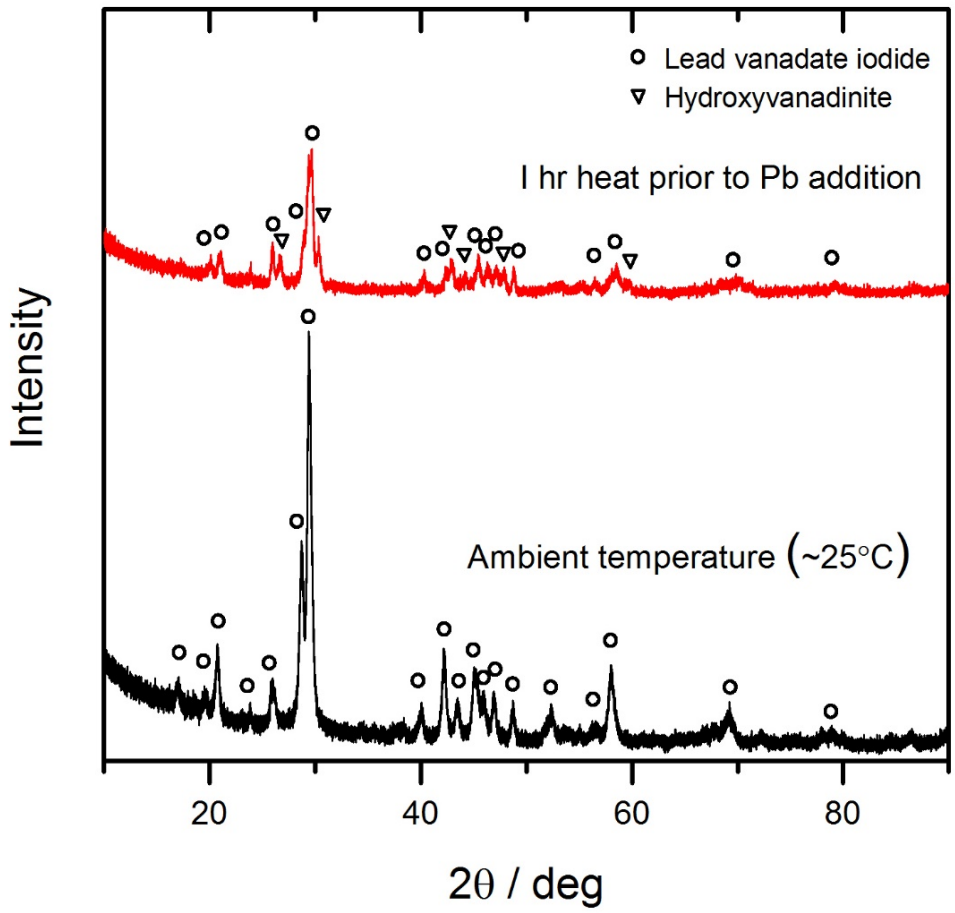

Figure 9. XRD pattern of lead vanadate iodide apatite with pre-heated VO_4/I solution and unheated VO_4/I solution

7.2 Glass Verification (in relation to section 6.1)

To ensure that all of the intended glasses were truly amorphous after the melt had cooled, x-ray diffraction was utilized to make sure there were no crystalline phases that were present in the material. X-ray diffraction patterns can be seen in Figures 10a-b.

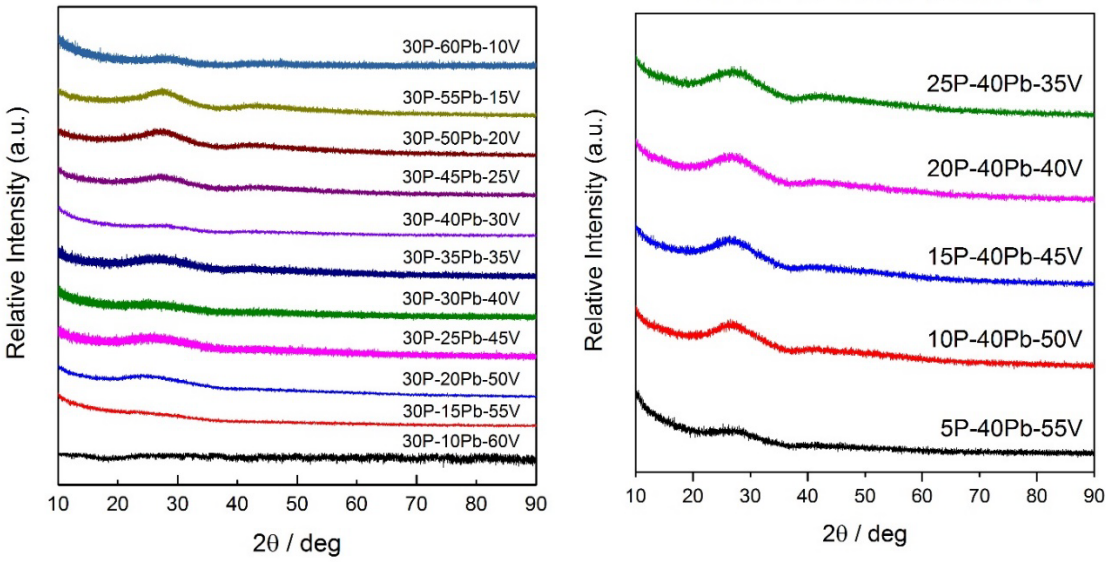

Figure 10a-b X-ray diffraction pattern of Series-1 (left) and Series-2 (right) of the proposed P-Pb-V glass binder series

8. References

1. 1. Energy Overview. *Monthly Energy Review* **2016**, 1-25.

2. Riley, B. J.; Vienna, J. D.; Strachan, D. M.; McCloy, J. S.; Jerden Jr, J. L., Materials and processes for the effective capture and immobilization of radioiodine: A review. *Journal of Nuclear Materials* **2016,** *470*, 307-326.

3. Michel, R.; Daraoui, A.; Gorny, M.; Jakob, D.; Sachse, R.; Tosch, L.; Nies, H.; Goroncy, I.; Herrmann, J.; Synal, H. A.; Stocker, M.; Alfimov, V., Iodine-129 and iodine-127 in European seawaters and in precipitation from Northern Germany. *Science of The Total Environment* **2012,** *419*, 151-169.

4. Riley, B. J.; Schweiger, M. J.; Kim, D.-S.; Lukens Jr, W. W.; Williams, B. D.; Iovin, C.; Rodriguez, C. P.; Overman, N. R.; Bowden, M. E.; Dixon, D. R.; Crum, J. V.; McCloy, J. S.; Kruger, A. A., Iodine solubility in a low-activity waste borosilicate glass at 1000 °C. *Journal of Nuclear Materials* **2014,** *452* (1–3), 178-188.

5. de Luis, R. F.; Martinez-Amesti, A.; Larrea, E. S.; Lezama, L.; Aguayoe, A. T.; Arriortua, M. I., Composite beta-AgVO3@V1.65+V0.44+O4.8 hydrogels and xerogels for iodide capture. *Journal of Materials Chemistry A* **2015,** *3* (39), 19996-20012.

6. Campayo, L.; Grandjean, A.; Coulon, A.; Delorme, R.; Vantelon, D.; Laurencin, D., Incorporation of iodates into hydroxyapatites: a new approach for the confinement of radioactive iodine. *Journal of Materials Chemistry* **2011,** *21* (44), 17609-17611.

7. Laurencin, D.; Vantelon, D.; Briois, V.; Gervais, C.; Coulon, A.; Campayo, L.; Grandjean, A., Investigation of the local environment of iodate in hydroxyapatite by combination of X-ray absorption spectroscopy and DFT modeling. *RSC Advances* **2014,** *4* (28), 14700-14707.

8. Coulon, A.; Laurencin, D.; Grandjean, A.; Coumes, C. C. D.; Rossignol, S.; Campayo, L., Immobilization of iodine into a hydroxyapatite structure prepared by cementation. *Journal of Materials Chemistry A* **2014,** *2* (48), 20923-20932.

9. Pei, C. Y.; Ben, T.; Xu, S. X.; Qiu, S. L., Ultrahigh iodine adsorption in porous organic frameworks. *Journal of Materials Chemistry A* **2014,** *2* (20), 7179-7187.

10. Pham, T. C. T.; Docao, S.; Hwang, I. C.; Song, M. K.; Choi, D. Y.; Moon, D.; Oleynikov, P.; Yoon, K. B., Capture of iodine and organic iodides using silica zeolites and the semiconductor behaviour of iodine in a silica zeolite. *Energy & Environmental Science* **2016,** *9* (3), 1050-1062.

11. Kato, H.; Kato, O.; Tanabe, H. In *Review of immobilization techniques of radioactive iodine for geological disposal*, International Symposium NUCEF 2001 - Scientific basis for criticality safety, separation process and waste disposal, Tokai, Ibaraki, Japan, Japan Atomic Energy Research Institute (JAERI): Tokai, Ibaraki, Japan, 2002; pp 697-704.

12. White, T.; Ferraris, C.; Kim, J.; Madhavi, S., *Apatite - An adaptive framework structure*. 2005; Vol. 57, p 307-401.

13. Kim, J. Y.; Fenton, R. R.; Hunter, B. A.; Kennedy, B. J., Powder diffraction studies of synthetic calcium and lead apatites. *Australian Journal of Chemistry* **2000,** *53* (8), 679-686.

14. Audubert, F.; Lartigue, J. E., Iodine Immobilization in Apatites. Scientific research on the back-end of the fuel cycle for the 21. century, 2000.

15. Cao, C.; Goel, A., Apatite Based Ceramic Waste Forms for Immobilization of Radioactive Iodine, An Overview. In *WM2016 Conference, March 6 - 10, 2016*, Phoenix, AZ, 2016.

16. Wang, J., Incorporation of iodine into apatite structure: a crystal chemistry approach using Artificial Neural Network. *Frontiers in Earth Science* **2015,** *3*.

17. Utsunomiya, S.; Yudintsev, S.; Wang, L. M.; Ewing, R. C., Ion-beam and electron-beam irradiation of synthetic britholite. *Journal of Nuclear Materials* **2003,** *322* (2–3), 180-188.

18. Lu, F. Y.; Yao, T. K.; Danon, Y.; Zhou, J. R.; Ewing, R. C.; Lian, J., Radiation Stability of Spark-Plasma-Sintered Lead Vanadate Iodoapatite. *Journal of the American Ceramic Society* **2015,** *98* (10), 3361-3366.

19. Merker, L.; Wondratschek, H., Bleiverbindungen mit Apatitstruktur, insbesondere Blei-Jod- und Blei-Brom-Apatite. *Zeitschrift für Anorganische und Allgemeine Chemie* **1959,** *300* (1/2), 41.

20. Audubert, F.; Carpena, J.; Lacout, J. L.; Tetard, F., Elaboration of an iodine-bearing apatite Iodine diffusion into a Pb3(VO4)2 matrix. *Solid State Ionics* **1997,** *95* (1–2), 113-119.

21. Sudarsanan, K.; Young, R. A.; Wilson, A. J. C., The structures of some cadmiumapatites' Cd5 (MO4) 3X. I. Determination of the structures of Cd5 (VO4) 3I, Cd5 (PO4) 3Br, Cd3 (AsO4) 3Br and Cd5 (VO4) 3Br. *Acta Crystallographica Section B: Structural Crystallography and Crystal Chemistry* **1977,** *33* (10), 3136-3142.

22. Wilson, A. J. C.; Sudarsanan, K.; Young, R. A., The structures of some cadmiumapatites' Cd5 (MO4) 3X. II. The distributions of the halogen atoms in Cd5 (VO4) 3I, Cd5 (PO4) 3Br, Cd5 (AsO4) 3Br, Cd5 (VO4) 3Br and Cd5 (PO4) 3Cl. *Acta*

Crystallographica Section B: Structural Crystallography and Crystal Chemistry **1977,** *33* (10), 3142-3154.

23. Baud, G.; Besse, J. P.; Sueur, G.; Chevalier, R., Structure de nouvelles apatites au rhenium contenant des anions volumineux: Ba10(ReO5)6X2 (X = Br, I). *Materials Research Bulletin* **1979,** *14* (5), 675-682.

24. Schriewer, M. S.; Jeitschko, W., Preparation and Crystal Structure of the Isotypic Orthorhombic Strontium Perrhenate Halides Sr5(ReO5)3X (X = Cl, Br, I) and Structure Refinement of the Related Hexagonal Apatite-like Compound Ba5(ReO5)3Cl. *Journal of Solid State Chemistry* **1993,** *107* (1), 1-11.

25. Phebe, D. E.; Narasaraju, T. S. B., Preparation and characterization of hydroxyl and iodide apatites of calcium and their solid solutions. *Journal of Materials Science Letters* **1995,** *14* (4), 229-231.

26. Flora, N. J.; Hamilton, K. W.; Schaeffer, R. W.; Yoder, C. H., A Comparative Study of the Synthesis of Calcium, Strontium, Barium, Cadmium, and Lead Apatites in Aqueous Solution. *Synthesis & Reactivity in Inorganic & Metal-Organic Chemistry* **2004,** *34* (3), 503-521.

27. Henning, P. A.; Lidin, S.; Petricek, V., Iodo-oxyapatite, the first example from a new class of modulated apatites. *Acta Crystallographica* **1999,** *55*, 165-169.

28. Audubert, F.; Savariault, J. M.; Lacout, J. L., Pentalead tris(vanadate) iodide, a defect vanadinite-type compound. *Acta Crystallographica Section C: Crystal Structure Communications* **1999,** *55* (3), 271-273.

29. Uno, M.; Shinohara, M.; Kurosaki, K.; Yamanaka, S., Some properties of a lead vanado-iodoapatite $Pb_{10}(VO_4)_6I_2$. *J. Nucl. Mater.* **2001,** *294* (1,2), 119-122.

30. Zhang, M.; Maddrell, E. R.; Abraitis, P. K.; Salje, E. K. H., Impact of leach on lead vanado-iodoapatite [Pb5(VO4)3I]: An infrared and Raman spectroscopic study. *Materials Science and Engineering: B* **2007,** *137* (1–3), 149-155.

31. Guy, C.; Audubert, F.; Lartigue, J.-E.; Latrille, C.; Advocat, T.; Fillet, C., New conditionings for separated long-lived radionuclides. *Comptes Rendus Physique* **2002,** *3* (7–8), 827-837.

32. Campayo, L.; Le Gallet, S.; Grin, Y.; Courtois, E.; Bernard, F.; Bart, F., Spark plasma sintering of lead phosphovanadate $Pb_3(VO_4)_{1.6}(PO_4)_{0.4}$. *Journal of the European Ceramic Society* **2009,** *29* (8), 1477-1484.

33. Yao, T.; Lu, F.; Sun, H.; Wang, J.; Ewing, R. C.; Lian, J., Bulk Iodoapatite Ceramic Densified by Spark Plasma Sintering with Exceptional Thermal Stability. *Journal of the American Ceramic Society* **2014,** *97* (8), 2409-2412.

34. Stennett, M. C.; Pinnock, I. J.; Hyatt, N. C., Rapid synthesis of Pb5(VO4)3I, for the immobilisation of iodine radioisotopes, by microwave dielectric heating. *J. Nucl. Mater.* **2011,** *414* (3), 352-359.

35. Lu, F.; Yao, T.; Xu, J.; Wang, J.; Scott, S.; Dong, Z.; Ewing, R. C.; Lian, J., Facile low temperature solid state synthesis of iodoapatite by high-energy ball milling. *RSC Advances* **2014,** *4* (73), 38718-38725.

36. Dong, Z. L.; White, T. J.; Wei, B.; Laursen, K., Model apatite systems for the stabilization of toxic metals: I, calcium lead vanadate. *Journal of the American Ceramic Society* **2002,** *85* (10), 2515-2522.

37. Kannan, S.; Lemos, A. F.; Ferreira, J. M. F., Synthesis and mechanical performance of biological-like hydroxyapatites. *Chemistry of Materials* **2006,** *18* (8), 2181-2186.

38. Bartholomäi, G.; Klee, W. E., The vibrational spectra of pyromorphite, vanadinite and mimetite. *Spectrochimica Acta Part A: Molecular Spectroscopy* **1978,** *34* (7), 831-843.

39. Griffith, W. P.; Wickins, T. D., Raman studies on species in aqueous solutions. Part I. The vanadates. *Journal of the Chemical Society A: Inorganic, Physical, Theoretical* **1966**, 1087-1090.

40. Shannon, R. D. t., Revised effective ionic radii and systematic studies of interatomic distances in halides and chalcogenides. *Acta Crystallographica Section A: Crystal Physics, Diffraction, Theoretical and General Crystallography* **1976,** *32* (5), 751-767.

41. Budavari, S.; O'Neil, M. J.; Smith, A.; Heckelman, P. E., *The merck index*. Merck Rahway, NJ: 1989; Vol. 11.